Materials Today Bio 28 (2024) 101199

Contents lists available at ScienceDirect

Materials Today Bio

journal homepage: www.journals.elsevier.com/materials-today-bio

Dual drug-loaded tumor-targeted polymeric nanoparticles for enhancing therapeutic response in pancreatic ductal adenocarcinoma

Naga Malleswara Rao Nakka [a,1], Hari Krishnareddy Rachamala [a,1], Ramcharan Singh Angom [a], Nagamalleswara Rao Indla [b,c], Shamit Kumar Dutta [a], Enfeng Wang [a], Santanu Bhattacharya [a,d], Annadanam V. Sesha Sainath [b,c], Hani Babiker [e], Krishnendu Pal [a], Debabrata Mukhopadhyay [a,d,*]

[a] Department of Biochemistry and Molecular Biology, Mayo Clinic College of Medicine and Sciences, Jacksonville, FL, 32224, USA
[b] Polymers and Functional Materials and Fluoro-Agrochemicals Department, CSIR-Indian Institute of Chemical Technology, Uppal Road, Hyderabad, 500007, India
[c] Academy of Scientific and Innovative Research (AcSIR), Ghaziabad, 201002, India
[d] Department of Physiology and Biomedical Engineering, Mayo Clinic College of Medicine and Sciences, Jacksonville, FL, 32224, USA
[e] Department of Medicine, Division of Hematology-Oncology, Mayo Clinic Florida, Jacksonville, FL, 32224, USA

ARTICLE INFO

Keywords:
Pancreatic ductal adenocarcinoma
Tumor-targeted therapy
Amphiphilic tri-block copolymer
Gemcitabine
Paclitaxel
Polymer nanoparticles

ABSTRACT

Pancreatic ductal adenocarcinoma (PDAC) is a lethal disease where standard-of-care chemotherapeutic drugs have limited efficacy due to the development of drug resistance and poor drug delivery caused by a highly desmoplastic tumor microenvironment. Combining multiple drugs in a tumor-targeting carrier would be a favorable approach to overcome these limitations. Hence, a tumor-targeted peptide (TTP) conjugated amphiphilic tri-block copolymer was developed to make targeted polymer nanoparticles (TTP-PNPs) serving as a vehicle for carrying gemcitabine (Gem), paclitaxel (PTX), and their combination (Gem + PTX). The TTP-PNPs in the form of empty polymer (P), single drug-loaded [P(Gem) and P(PTX)], and dual drug-loaded [P(Gem + PTX)] polymer nanoformulations exhibited stable and homogenous spherical shapes with 110–160 nm size. These nanoformulations demonstrated excellent stability under *in vitro* physiological conditions and led to an efficient release of the drugs in the presence of reduced glutathione (GSH). The efficacy of these nanoparticles was thoroughly evaluated *in vitro* and *in vivo*, demonstrating a notable capacity to selectively target and restrict PDAC cells (PANC-1 and KPC) growth. The cellular uptake and biodistribution study showed a significantly higher tumor-targeting ability of TTP-PNPs than PNPs without TTP. Notably, P(Gem + PTX) exhibited the lowest IC_{50} compared to all other controls and showed heightened synergistic effects in both cell lines. Furthermore, P(Gem + PTX) showed a significantly better tumor reduction and median overall survival in mouse models than single drug-loaded TTP-PNPs or a combination of free drugs (Gem + PTX). In summary, our TTP-PNP system shows great promise as a novel platform for delivering Gem + PTX specifically to pancreatic cancer (PC), maximizing the therapeutic benefits with lower concentrations of the drugs and potentially reducing toxic side effects.

1. Introduction

PDAC is the third most common cause of cancer-related deaths in the United States, with a relatively low 5-year survival rate of around 12.5 % in 2024 [1]. Surgical resection of the tumor is a viable treatment option. Still, it can only cure a small percentage (15 %) of patients who are diagnosed at an early stage with resectable and borderline resectable PDAC [2]. Unfortunately, most PDAC patients are diagnosed with advanced local stage or distant metastatic form of the disease, making palliative chemotherapy the only treatment approach [3,4].

The use of single chemotherapeutic agents is limited by poor stability and bioavailability, systemic toxicity, severe side effects, and drug resistance [5,6]. Instead of single-agent chemotherapy, a multi-drug chemotherapeutic regimen approach has become the mainstay of treatment to enhance combined delivery and overcome resistance [2,7,8].

* Corresponding author. Department of Biochemistry and Molecular Biology, Mayo Clinic College of Medicine and Sciences, Jacksonville, FL, 32224, USA.
E-mail address: Mukhopadhyay.debabrata@mayo.edu (D. Mukhopadhyay).
[1] Both authors contributed equally.

https://doi.org/10.1016/j.mtbio.2024.101199
Received 6 April 2024; Received in revised form 5 August 2024; Accepted 9 August 2024
Available online 10 August 2024

Gemcitabine monotherapy, the initial standard of care treatment for PDAC, exhibited modest efficacy with minimal improvement in overall response rate, progression-free survival, and overall survival (OS), yet led to side effects specifically in elderly patients. Hence, to improve treatment outcomes, investigators explored the combination of Gem with other chemotherapeutic agents [9,10]. In 2013, the FDA approved albumin-bound PTX (nab-PTX) for treating PDAC in combination with Gem. In a large-scale phase III clinical trial, the nab-PTX-Gem cohort, with an approximately 10:1 w/w ratio of Gem/PTX, demonstrated an improved OS compared to the control arm, a single-agent Gem [11,12]. However, the treatment resulted in a high percentage of side effects, with leukopenia, neutropenia, fatigue, and peripheral neuropathy. These findings demonstrated that combining Gem and nab-PTX can improve efficacy and increase toxicities [12,13].

To address this challenge, the development of nanocarrier-based drug delivery systems such as inorganic metal nanoparticles, liposomes, and polymeric nanoparticles has become a more promising and novel drug delivery treatment approach that can increase efficacy by overcoming the pharmacokinetic limitations of anti-cancer drugs and also maintain an appropriate balance between efficacy and toxicity [14–17]. Moreover, nanoparticles can be modified to target active tumors effectively by attaching tissue-specific ligands to their surfaces. These ligands can be different molecules, such as antibodies, peptides, aptamers, and vitamins [18–20]. Targeted drug delivery using targeting ligands against overexpressed receptors in tumor tissue offers several advantages over without-targeted counterparts, including precise delivery of drug-loaded nanoparticles, enhanced drug accumulation, and increased cellular uptake at tumor sites [3]. Tumor-targeted peptide--conjugated polymer nanoformulations with hydrophilic and hydrophobic blocks, also known as targeted amphiphilic copolymers, are some of the most innovative investigated nanocarriers [21,22]. The significant potential has been demonstrated by these copolymers in nanomedicine for their ability to enhance drug delivery to the targets through improved drug bioavailability and balanced pharmacokinetics of hydrophilic and hydrophobic drugs [23,24]. They can achieve synergistic therapeutic effects through a simultaneous treatment approach [25].

Fibroblast growth factor receptor 1 (FGFR1) is a receptor tyrosine kinase (RTK) that, along with fibroblast growth factors (FGFs), plays a role in transmitting signals across the plasma membrane, controlling cell migration, proliferation, and apoptosis. Abnormal function of this receptor can lead to developmental disorders and is found in many types of cancer, including PDAC. FGFR1 presents potential binding sites for targeting molecules and can be efficiently internalized for intracellular drug delivery. The structure of our tumor-targeting peptide (TTP) on a previously published peptide sequence that was shown to bind FGFR1. It can be used as a pan-tumor targeting agent in several indications. It is an appealing target for selective anticancer therapies, but novel FGFR1-targeting molecules are still needed to improve drug delivery efficiency and selectivity [26–28].

Previously, we demonstrated that co-delivery of Gem and PTX systemically using a targeted peptide-decorated liposomal formulation caused significantly higher reductions in tumor growth in PDAC than without TTP formulations loaded with Gem or PTX [29]. Targeted peptide-coated gold nanoparticles were utilized to deliver Gem systemically in mice with PC. This resulted in significantly higher cytotoxicity observed *in vitro* and an impressive antitumor ability in a PANC-1 orthotopic xenograft model. The nanoparticles were selectively taken up in the PDAC tumor tissues, thus demonstrating a promising strategy for treating PC [30]. However, in both instances, the stability of the nanoformulation and drug loading efficiency and reproducibility were not optimal.

Therefore in this present work, the FGFR1-targeting peptide is used as a TTP. It is conjugated Polyethylene glycol-*b*-Poly(N-Vinyl caprolactam-*co*-hydroxyethyl acrylate-*g*-lipoic acid) [TTP-PEG_6-*b*-P(NVCL-*co*-HEA-*g*-LA)] nanocarrier is used for active targeted co-delivery of Gem and PTX to the PDAC. The physicochemical properties, encapsulation efficiency, loading content, and release profile of the polymer nanoformulation are thoroughly investigated. As part of the biological evaluation, *in vitro* cellular uptake, cytotoxicities, *in vivo* biodistribution, tumor growth inhibition, and survival are assessed. The dual drug-loaded polymer nanoformulation significantly inhibited tumor growth and increased survival in orthotopic pancreatic tumor models using lower drug doses than typically administered [31,32]. In summary, our results demonstrate that the described tumor-targeted polymer nano drug delivery system has considerable therapeutic potential in PDAC.

2. Materials and methods

2.1. Materials

N-Vinyl caprolactam (NVCL), 1,4-dioxane, anhydrous dichloromethane 98 %, 4-cyano-4-(phenyl carbonothioylthio) pentanoic acid (CTA-COOH), lipoic acid (LA) 98 %, N, N, N′, N' tetramethyl-O-(benzotriazole-1-yl) uranium hexafluorophosphate (HBTU), 1-hydroxy benzotriazole hydrate (HOBt), and *N*, *N*-diisopropylethylamine (DIPEA) and azo-bis-isobutyronitrile (AIBN). Additionally, GSH and dialysis tubing of cellulose membrane (MW cut-off ¼ 3500) were purchased from Millipore Sigma. Furthermore, 97 % 2-hydroxyethyl acrylate (HEA) was obtained from Thermo Scientific, and *t*-Bu–OOC–PEG_6-OH was purchased from Nano soft polymers. The AIBN and NVCL recrystallization process was repeated twice, using methanol and n-hexane as solvents respectively. Resulted crystals were dried under vacuum at 35 °C for 10 h and stored at 4 °C. HEA was purified by distillation. The buffer solution was prepared with an analytical grade. Gem and PTX were procured from LC Laboratories, MA, USA. Pen-Strep solution and DMEM media were purchased from Gibco, USA. Fetal bovine serum (FBS) was purchased from Gemini Bioproducts, USA. Milli Q water was used for all the experiments.

2.2. Methods

Synthesized polymers were characterized by Fourier transform infrared (FT-IR) (Thermo Net al.670 spectrometer) spectroscopy at a resolution of 4 cm^{-1} using the KBr sampling method at room temperature (single averaged 35 scans). The polymer proton nuclear magnetic resonance spectroscopy (^{1}H NMR) was documented on AVANCE-400 or INOVA-500 spectrometer in the $CDCl_3$ (Aldrich) material solution with tetramethyl silane as an internal standard. The Gem and PTX-loaded PNPs' size, polydispersity index (PDI), and zeta potential were determined using the dynamic light scattering (DLS) method (Zetasizer Nano ZS, Malvern, UK) at 25 °C. Before the measurement, all samples were diluted with water to appropriate dilutions to resolve these parameters. The Gem and PTX encapsulation efficiencies were determined by UV–Vis spectrometry (UV-2401 PC, USA). The morphological properties of the PNPs were checked by Transmission electron microscopy (TEM). It was performed using a Tecnai G220 TEM at an accelerating voltage of 120 kV. TEM samples were prepared by dropping 10 μL of 0.2 mg/mL PNPs solution on the copper grid and staining them with uranyl acetate (3 wt%) [33].

2.3. Experimental

2.3.1. Preparation of PEG_6-based reversible addition fragmentation chain transfer (RAFT) macro-initiator (PEG_6-CTA)

Esterification of CTA-COOH with hydroxy-PEG_6-*t*-butyl ester using a simple DCC/DMAP esterification method [34].

2.3.2. Preparation of Poly(ethylene glycol)-b-poly(N-vinyl caprolactam-co-hydroxyethyl acrylate) [^{t}but–OOC–PEG_6-b-P(NVCL-co-HEA)]

A mixture of NVCL (3 g, 21.02 mmol), 2-hydroxyethyl acrylate (HEA) (0.7 g, 15.2 mmol), AIBN (10 mg, 1.18 mmol) and PEG_6-CTA RAFT agent (80 mg, 1. 58 mmol) in 10 mL of dry 1,4-dioxane were

added in 50 mL round bottom flask. The polymerization reaction mixture was degassed using freeze-pump-thaw process cycles three times under a nitrogen atmosphere. Subsequently, the round bottom (RB) flask was sealed and rested for 24 h in a pre-heated 90 °C with a stirrer. The polymerization was terminated by adding 0.5 mL of methyl alcohol (MeOH), air-exposed, and then precipitated in cold ether twice. Finally, the resulting PEG block copolymer, ^{t}But–OOC–PEG$_6$-*b*-P(NVCL-*co*-HEA), was formed and dried at 60 °C for 48 h beneath vacuum.^{1}H NMR (400 MHz, $CDCl_3$) δ 7.38, 7.379, 4.86, 4.61, 4.45–4.40, 4.18, 3.97–3.77, 3.65–3.57, 3.16, 2.98–2.85, 2.62–2.49, 2.33–2.17, 1.74–1.51 and 1.33 ppm. FT-IR: 3429.16 (OH), 2933.98, 2861.35 (-CH), 1729.96 (-O-C=O), 1624.13 ((-N-C=O) 1481.73, 1446.58, 1395.15, 1264.48, 1194.21, 1082.63, 976.23 and 755.05 cm^{-1}.

2.3.3. Preparation of Poly(ethylene glycol)-b-poly(N-vinyl caprolactam-co-hydroxyethyl acrylate-g-lipoic acid) [HOOC-PEG$_6$-b-P(NVCL-co-HEA-g-LA)]

LA (2.77 g, 13 mmol), PEG block copolymer (1.66 g, 8.3 mmol), and DMAP (1.02 g, 8.3 mmol) were dissolved in dry DCM (20 mL) in an RB flask and cooled under stirring over ice for 10 min. DCC (3.36 g, 16 mmol) dissolved in DCM (20 mL) was added dropwise to the mixture. The reaction mixture was kept on ice for 30 min and left at room temperature for 5 h, followed by *t*-butyl group deprotection with 10 % TFA. The crude mixture was precipitated in diethyl ether three times and the resultant HOOC-PEG$_6$-*b*-P(NVCL-*co*-HEA-*g*-LA) was dried under reduced pressure and stored at 4 °C. Mn = 11890 g/mol ^{1}H NMR (500 MHz, $CDCl_3$) δ 7.40, 5.86, 4.73–4.54, 4.46, 4.20, 4.14, 3.89–3.79, 3.66–3.55, 3.43–3.39, 3.24–3.18, 2.68–2.50, 2.23–2.15, 1.76–1.53, 1.26 and 0.90 ppm. FT-IR: 3426.78 (OH), 2930.33, 2860.15 (-CH), 1731.41 (-O-C=O), 1646.11 (-N-C=O)1566.46, 1446.09, 1396.29, 1166.32, 1081.07 and 812.03 cm^{-1}.

2.3.4. Preparation of tumor targeted peptide conjugated-Poly(ethylene glycol)-b-poly(N-vinyl caprolactam-co-hydroxyethyl acrylate-g-lipoic acid). [TTP-PEG$_6$-b-P(NVCL-co-HEA-g-LA)]

The TTP was conjugated with PEG-block copolymer via solid phase coupling. Briefly, TTP-loaded resin (200 mg) was taken into the 250 mL reactor, and then HOOC-PEG$_6$-*b*-P(NVCL-*co*-HEA-*g*-LA) (2 equiv.), HBTU (2 equiv.), HOBt (2 equiv.) and DIPEA (4 equiv.) in DMF were added to the reactor at room temperature for 6 h. TTP-loaded resin was prepared following the same procedure as described previously [33,35]. The final TTP-polymer was obtained by dissolving the peptide-conjugated polymer in 2 mL methanol, precipitating it in cold ether, and drying it under reduced pressure, after which it was stored at 4 °C for further use. ^{1}H NMR (500 MHz, $CDCl_3$) δ 8.83–8.46, 8.36, 7.79–7.36, 7.19, 6.80, 5.90–5.87, 5.54, 5.17, 4.66–4.54, 4.36–4.29, 4.21–4.02, 3.78–3.63, 3.52, 3.40–3.22, 3.17–3.14, 2.58–2.48, 2.33, 2.21–2.07, 1.80–1.72, 1.66–1.59, 1.53–1.40, 1.38–1.25 and 0.89 ppm. FT-IR: 3421.93 (OH), 2936.92, 2739.2 (-CH), 2678.03, 2491.91, 1747.24 (-O-C=O), 1628.45 (-N-C=O) 1454.30, 1368.68, 1199.75, 1096.71, 1039.90, 976.37 and 820.19 cm^{-1}.

2.3.5. Preparation of gemcitabine and paclitaxel-loaded PNPs

PTX-loaded polymeric nanoparticles P(PTX) (NPs) were prepared using the nanoprecipitation process [36]. Briefly, 10 mg of the polymer [TTP-PEG$_6$-*b*-P(NVCL-*co*-HEA-*g*-LA)] and 1 mg of paclitaxel were dissolved in 200 μL of dichloromethane (DCM). Then, the DCM solution was slowly dripped into 2 mL of an aqueous solution containing a mixture of 0.5 % DSPE-PEG$_{2000}$-OMe. The mixture was magnetically stirred at room temperature overnight at 500 rpm to evaporate the organic solvent. The resulting nanoparticle solution was centrifuged at 10000 rpm for 15 min using 3.5 K MWCO Amicon filter tubes and washed thrice with water to remove unencapsulated paclitaxel. Gemcitabine-loaded P(Gem) and dual drug-loaded P(Gem + PTX) PNPs were also prepared using the same procedure. Drug-free nanoparticles (empty polymeric NPs) were also prepared similarly without adding gemcitabine and paclitaxel. DLS and TEM are used to analyze the sizes and morphology of PNPs.

2.3.6. Entrapment efficiency (EE %) and drug loading efficiency (DLE %) of PNPs

As previously reported, the UV–Vis spectrometry analysis measured the drug loading content (DLE) [29]. First, the standard curves for gemcitabine and paclitaxel ranging from 10 to 100 μg/mL were determined using UV–Vis spectroscopy. The absorbance was measured at 275 and 230 nm, respectively. The Gem and PTX concentrations in PNPs were calculated by comparing the absorbance of Gem and PTX in the standard calibration curve. The measurement was repeated thrice.

The EE % and DLE % of Gem and PTX are calculated as follows:

EE %= (amount of drug entrapped in NPs/initial amount of drug added) X 100 % and DLE %= (amount of drug entrapped in NPs/weight of freeze-dried NPs) X 100 %

2.3.7. TTP-PNPs stability study

To evaluate the *in vitro* stability of NPs, empty PNPs, and Gem and PTX-loaded P(Gem + PTX) NPs were stored at 4 °C in water for up to 30 days. The hydrodynamic size of the particles was measured at regular intervals to determine the stability of the formulation.

2.3.8. In vitro drug release studies

A dialysis method was used to evaluate the drug release efficiency of polymer nanoparticles. It is known that the concentration of GSH in the blood is minimal (1–2 μM) [37], but it is nearly 10^3 times higher (2–10 mM) in the cellular cytoplasm. In this experiment, A suspension of PNPs containing approximately 440 μg of Gem and 820 μg of PTX was prepared in 3 mL of PBS. The suspension was placed in a dialysis bag with a molecular weight cut-off of 3.5 kDa. The bag was immersed in 10 mL of 0.5 % Tween in PBS with or without 10 mM GSH [38]. An orbital shaker was set at 300 rpm and maintained at 37 ± 0.5 °C for 24 h. Every hour, 1 mL of dialysate was collected and replaced with an equal volume of PBS to maintain sink conditions. The amount of PTX and Gem released from the NPs was analyzed using UV–Vis spectroscopy.

$$\textit{Cumulative released drug}\ (\%) = (\textit{Weight of released drug in medium}\ (\mu g)) / (\textit{Weight of loaded drug in to polymer nanoparticles}\ (\mu g)) \times 100$$

2.3.9. Cell culture

PANC-1 human-derived pancreatic cancer cell line (obtained from ATCC USA), and KPC murine pancreatic cancer cells derived from the transgenic KrasLSL.G12D/+; p53R172H/+; PdxCretg/+ C57BL/6 mouse was a gift from one of our collaborators (Dr. Sunil Krishnan, Mayo Clinic, Jacksonville, Florida) were cultured in DMEM medium supplemented with 10 % FBS. primary endothelial cell lines, Human Umbilical Vein Endothelial Cells (HUVEC), and human pancreatic ductal endothelial cells (HPDECs) were cultured in our previously published protocol [39]. All the cell lines were maintained at 37 °C with 5 % CO_2 in a humidified chamber.

2.3.10. In vitro cellular uptake of polymer nanoparticles

Cellular uptake was investigated using a confocal microscope with fluorescent Rhodamine-B-loaded targeted or without TTP-PNPs prepared in the same manner described previously in the PNPs preparation section. PANC-1 and KPC cells were seeded in a chamber slide at 2×10^4 cells/well. After 24 h incubation, these cells were treated with rhodamine-loaded targeted and without-TTP-PNPs formulations for two time points, 2 and 4 h. After that, the cells were washed with PBS (pH 7.4) three times and then fixed using 4 % paraformaldehyde. The nuclei of the cells were counterstained with DAPI for the last 30 min. The cells were imaged in a Zeiss confocal microscope (LSM 880) using blue (Alexa

405), and red (Alexa 594) channels.

2.3.11. In vitro cytotoxicity study

The *in vitro* cytotoxicities of free drugs and drug-load polymeric nanoparticles were evaluated at concentrations ranging from 600 nM to 4 μM and 300 nM to 2 μM with respect to PTX and Gem, respectively, for 72 h using the MTS assay. Initially, PANC-1 and KPC (5×10^3) cells were seeded in 100 μL of DMEM medium in 96-well plates and cultured overnight. The medium was then replaced with fresh medium containing different concentrations of Gem and PTX and single and dual drug-loaded polymer nanoparticles. The control group did not receive any treatment. After 72 h, cell viability was measured by incubating cells with 10 μL MTS (10 mg/mL) for 1 h at 37 °C. The absorbance at 492 nm was measured using Spectra Max i3x. The experiment was performed in triplicate. Similarly, 24 h cytotoxicity was compared between PANC-1 and noncancer cells such as HUVEC and HPDEC.

Percentage viability is calculated as follows:

$$\text{Viability } (\%) = 100 \text{ x } (A_{\text{Treated}} - A_{\text{Blank}})/(A_{\text{Untreated}} - A_{\text{Blank}}).$$

2.3.12. Calculation of the combination index

Our study examined the combination index (CI) of administering PTX and Gem together as a therapeutic approach [40]. We used a formula based on the IC_{50} values from the MTS assay to calculate the CI, which helps determine the overall outcome of the treatment. When a CI is greater than 1, it indicates antagonistic behavior, a CI of 1 corresponds to additive behavior, and a CI less than 1 represents synergistic behavior.

$$\text{CI} = \frac{IC_{50}(X+Y)}{IC_{50}(X)} + \frac{IC_{50}(X+Y)}{IC_{50}(Y)}$$

where: $IC_{50}(X) = IC_{50}$ of (Gem)/P(Gem) and IC_{50} (Y) = IC_{50} of (PTX)/P (PTX) are the IC_{50} values obtained from each drug separately. IC_{50} (X + Y) =IC_{50} of (Gem + PTX)/P(Gem + PTX) is the IC_{50} value of both drugs in combination.

2.3.13. Orthotopic tumor cell implantation on SCID and C57BL/6J mice

SCID and C57BL/6J mice were acquired from the Jackson Laboratory, USA. The animal work was conducted following the guidelines of the Association for Assessment and Accreditation of Laboratory Animal Care (AAALAC) and approved by the Mayo Clinic Institutional Animal Care and Use Committee (IACUC) protocols.

"The orthotopic tumor cell implantation was performed following previously published protocol [41,42]. Briefly, before performing orthotopic tumor cell implantation on SCID and C57BL/6J mice, they were anesthetized with ketamine/xylazine administered intraperitoneally. The fur on the left dorsal area was shaved and sterilized with iodine solution and 70 % alcohol. The hind paw was pinched to confirm full anesthesia, and if no response was observed, the animal was considered ready for surgery. Approximately $2 \times 10^{*6}$ GFP-Luciferase-labeled PANC-1 cells and $5 \times 10^{*4}$ luciferase-transfected KPC cells in 100 μl sterile 50 % matrigel in PBS were loaded into a 1.0 mL sub-Q syringe with a 26G needle. The general area of the spleen (left upper quadrant of the abdomen) was located, and with forceps, the skin on top of that region was pinched. A 1.0 cm incision was made with surgical scissors to create a pocket, and the smooth muscle on top of the spleen was pinched and cut through to access the peritoneal cavity. The caudal end of the spleen was gently grabbed and pulled out of the body, with the pancreas attached to it. The pancreas was spread using a wet sterile Q-tip, and the head of the pancreas was located. The 50 μl injection was delivered into the head of the pancreas, leaving the needle inside for 10 s and then slowly rotating the needle out of the pancreas. A successful implantation was visually confirmed as a superficial bubble without any leaks. The pancreas and spleen were then returned to the peritoneal cavity, with the muscle and skin separately enclosed using a suture. Following the injection, the mice were transferred to their cage and kept under a heating lamp for recovery. Analgesia was administered to the mice from 2 days pre-surgery to 3 days post-surgery. The mice were observed daily, and treatment started 3 and 1 weeks after implantation of PANC-1 and KPC, respectively.

2.3.14. In vivo tumor-targeting evaluation

Male SCID mice, aged six to eight weeks, were acquired from the in-house breeding program and were kept in institutional animal facilities. The tumor-targeting efficiency of our targeted polymer nanoformulation was evaluated by establishing tumor-bearing models through orthotopic injection of 2×10^6 GFP-Luciferase-labeled PANC-1 cells. After three weeks, when the tumors became palpable, mice were imaged using IVIS by bioluminescence imaging. Mice having similar luciferase signals were randomly divided into four groups (n = 3): i) control, ii) NiR dye, iii) without-targeted PNPs (CP), iv) targeted PNPs (TP), with 1 mg/kg NiR dye administered via intravenous injection (i.v). After 24 h after administration, the mice were anesthetized and imaged using IVIS (Caliper et al., USA). Then, the mice were euthanized, and major organs were collected and imaged in ex vivo to validate the increased targeting efficiency.

2.3.15. In vivo antitumor efficacy and survival study

The effectiveness of various PNPs in treating tumors was evaluated in both PANC-1 xenografts and syngeneic KPC models. To perform the experiment, GFP-Luciferase-labeled 2×10^6-PANC-1 and 5×10^4 KPC cells were injected into the head of the pancreas of female SCID and C57BL/6J mice aged 8–10 weeks, respectively. After three weeks of PANC-1 tumor cell and one week of KPC cell implantation, the mice were imaged using IVIS by bioluminescence imaging. Mice having similar luciferase signals were randomly divided into five groups (n = 5): i) control only PNPs, ii) free drugs gemcitabine and paclitaxel (Gem + PTX), iii) poly paclitaxel [P(PTX)], iv) poly gemcitabine, [P(Gem)], and v) poly gemcitabine plus paclitaxel [P(Gem + PTX)]. Treatments were administered twice weekly for three weeks via intravenous and (i.v) injection, and body weights were also measured total 4 times for 3 weeks. Two days after the final treatment, the mice were euthanized, and their tumors, along with major organs such as hearts, livers, spleens, lungs, and kidneys were harvested. The tumors were weighed and measured in volume using calipers. We used formula V = ½ ($a \times b^2$) to calculate the tumor volumes, where a and b represent the longest and shortest diameters, respectively. Additionally, we conducted a survival study on mice with PANC-1 and KPC tumors to determine the median survival enhancement. After treatment, we recorded each mouse's survival termination date as the IACUC endpoint.

2.3.16. Immunohistochemistry

Tumors and organs were fixed in 10 % formalin buffer at room temperature for 24 h before embedding in paraffin for sectioning. Sections were deparaffinized and exposed to hematoxylin, eosin (H&E), and Ki67 immunochemistry according to the manufacturer's instructions (DAB 150; Millipore). Stable diaminobenzidine and hematoxylin were used as the chromogen substrate and the counterstain, respectively. Photographs of cross sections were digitalized with the Aperio AT2 slide scanner (Leica). Images were analyzed using ImageScope software (Leica).

2.4. Statistical analysis

The experiments were conducted four times independently, and the statistical analysis was performed using GraphPad Prism 10.0.2 (GraphPad et al., USA). The results were presented as the mean ± standard deviation. To compare the groups, we used a one-way analysis of variance (ANOVA), and a p-value of <0.05 was considered statistically significant.

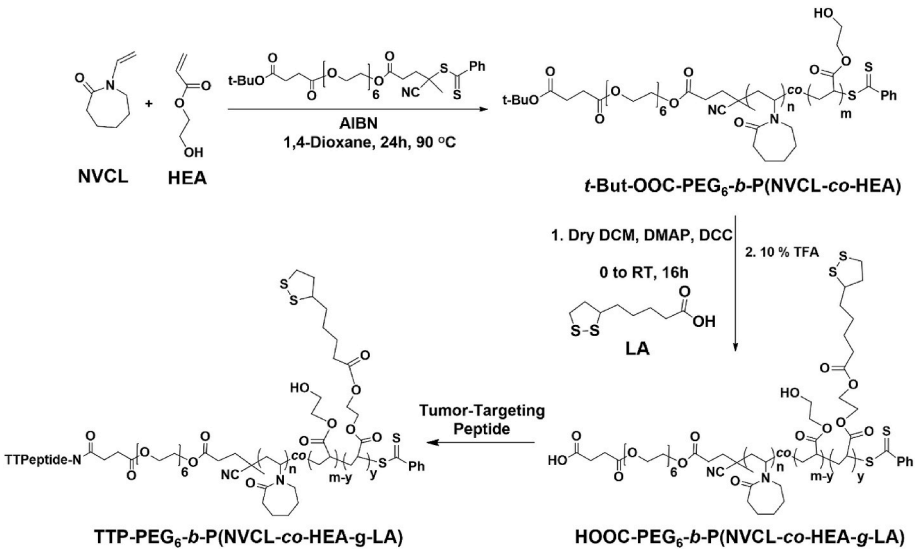

Scheme 1. Synthesis of tumor-targeted peptide conjugated amphiphilic triblock copolymer (TTP-PEG_6-*b*-P(NVCL-*co*-HEA-*g*-LA) via RAFT Polymerization.

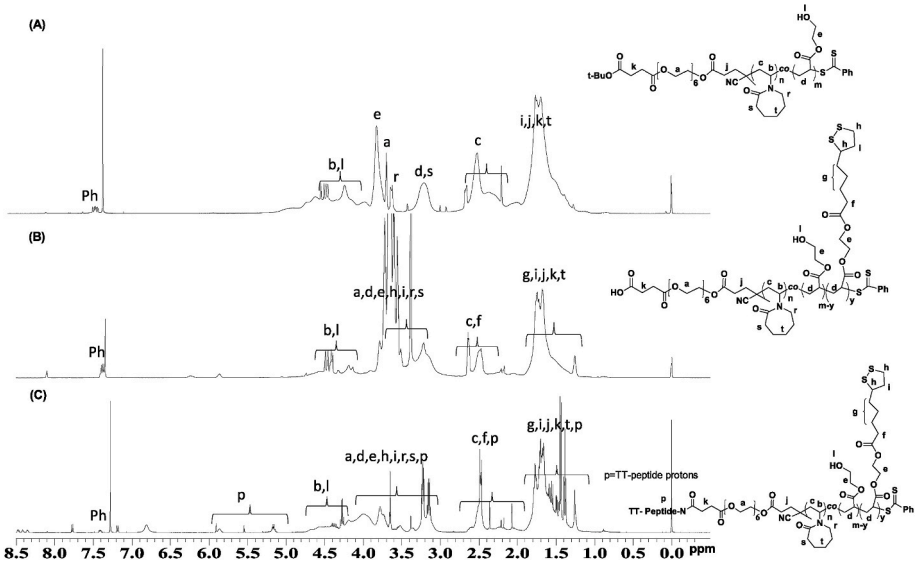

Fig. 1. ^{1}H NMR spectra of **(A)** *t*-But–OOC–PEG_6-*b*-P(NVCL-*co*-HEA), **(B)** HOOC-PEG_6-*b*-P(NVCL-*co*-HEA-*g*-LA) and **(C)** TTP-PEG_6-*b*-P(NVCL-*co*-HEA-g-LA).

3. Results and discussion

3.1. Polymer synthesis and design rationale

We have engineered a tumor-targeted peptide conjugated amphiphilic block copolymer such as TTP-PEG_6-*b*-P(NVCL-*co*-HEA-*g*-LA) synthesized using RAFT copolymerization. It polymerizes the monomer system, allowing precise control of the final polymer structure. The TTP-copolymer consists of an FGFR1-targeting peptide, and its structure is based on a previously published peptide sequence that was shown to bind FGFR1 [26,35,43], a hydrophilic PEG block, a P(HEA) core, and a lipophilic and stimulative or thermo-responsive P(NVCL) core. The PEG and P(HEA) core enhances the copolymer's biocompatibility and solubility. Additionally, the P(HEA) block is grafted with LA to increase hydrophobicity and stabilize the polymer nanoformulation. The targeted peptide is also conjugated with PEG on the other end. The P (NVCL), P(HEA), and LA blocks are chosen for their biocompatibility and protein-repellent nature, ensuring the carriers can circulate in the bloodstream for an extended period with minimum opsonization [44]. This emphasizes the safety and effectiveness of the carriers.

3.2. Preparation and characterization of targeted peptide conjugated PEG-block copolymer

We have successfully synthesized and characterized a TTP-conjugated amphiphilic triblock copolymer, such as TTP-PEG_6-*b*-P (NVCL-*co*-HEA-*g*-LA), in three steps. The polymerization of NVCL and HEA was stopped before the total conversion of monomers to retain the RAFT end-group functionality. In the first step, ^{t}Bu–OOC–PEG_6-CTC, RAFT agent was used along with AIBN as an initiator to polymerize NVCL and HEA using the RAFT method at 90 °C for 24 h to obtain ^{t}Bu–OOC–PEG_6-*b*-P(NVCL-*co*-HEA). The obtained polymer was then post-modified with LA by esterification, followed by deprotection of the t-butyl group with 10 % TFA (Trifluoroacetic acid) to obtain HOOC-PEG_6-*b*-P(NVCL-*co*-HEA-*g*-LA) in the second step. In the third step, the polymer obtained in step two was used for targeted peptide conjugation (TTP-PEG_6-*b*-P(NVCL-*co*-HEA-*g*-LA), as shown in Scheme 1. The successful synthesis of the targeted polymer was characterized by using ^{1}H NMR, gel permeation chromatography (GPC), and FT-IR spectroscopy techniques, providing us with a solid foundation for further research and development.

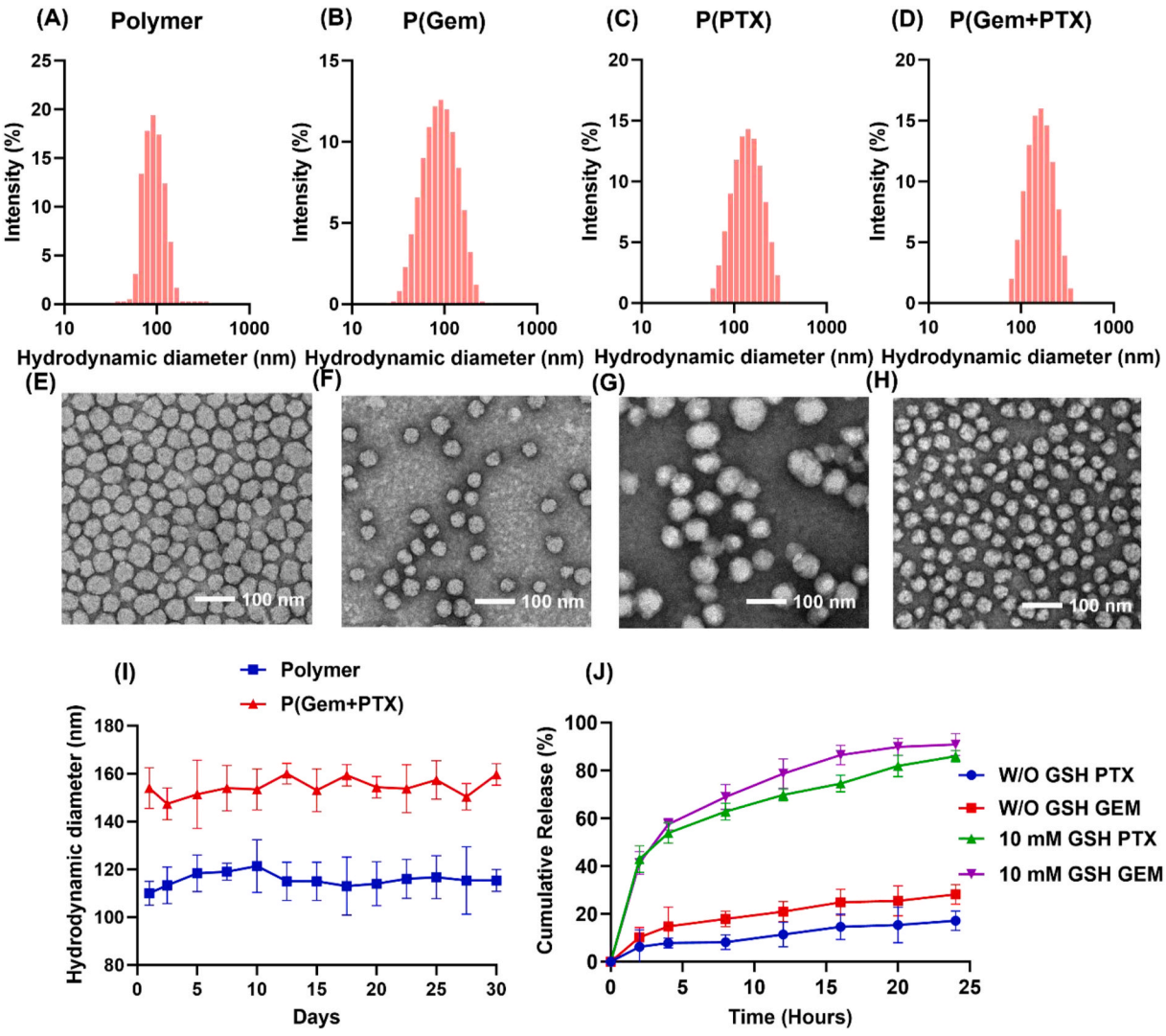

Fig. 2. The physical characteristics of single and dual drug-loaded polymer nanoparticles. The hydrodynamic diameter histograms of the polymer nanoparticles were obtained through DLS intensity measurement. The morphology of transmission electron micrographs with a scale bar of 100 nm was examined for four types of nanoparticles: (**A&E**) empty polymer (P), (**B&F**) P(Gem, **(C&G)** P(PTX), and (**D&H**) P(Gem + PTX). (**I**) Stability of the empty polymer and dual drug-loaded polymeric nanoparticles and (**J**) Cumulative drug release with and without (W/O) GSH. All the measurements were performed in deionized water at 25 °C.

The typical ^{1}H NMR characterization in Fig. 1(A–C) showed that all the proton signals of P(NVCL), P(HEA), LA, and TTP were highly correlated with their molecular structures. P(NVCL) group characteristic peaks proton signals at δ 4.45 (1H, -N-CH), δ 3.65 (2H, –NCH_2–), δ 3.16 (2H, –$COCH_2$–), δ 2.33–2.17 [-CH_2 – of the backbone from P(NVCL)] and δ 1.74–1.51 ppm (6H, –CH_2– of the caprolactam ring). The δ 4.86–461 ppm corresponding to P(HEA) block signal and the of the proton from the hydroxyl group appeared at δ 3.97–3.77 (4H –O–CH_2), P (HEA) polymer backbone -O-CH2- singles appeared at δ 3.24–3.18 and 3.7 ppm from -O–CH_2– PEG block, in the triblock copolymer, Similar step-2 and 3 conformed by ^{1}H NMR spectrum (Fig. 1B and C). PEG, P (NVCL), and P(HEA) proton peaks along with new peaks appeared at δ 3.44–3.39 (-S-CH_2), δ 2.60–250 (2H, –$COCH_2$–), and δ 1.2–1.8 ppm (6H -CH_2- protons from the long chain from LA and targeted peptide merged with copolymer protons from δ 6.80 δ 5.90–5.87, δ 4.21–4.02, δ 3.4–3.22 ppm and δ 1.38–1.25 ppm corresponding to -C-H, -N-H, and –C=O–NH protons. The GPC traces of Step-2 (Fig. S1) showed that number average molecular weight (Mn) was 1.19×10^4, and the PDI was 1.34.

The FT-IR spectrum of step-1 showed characteristic strong bands in signal, 2933.98 cm^{-1} from -C-H, 2861.35 cm^{-1} stretch from PEG, P (NVC) block 3429.16 cm^{-1}, and 1729.96 cm^{-1} for the stretch OH and -O-C=O group from the PHEA block, and -N-C=O ester bond cyclic amide stretch from P(NVCL) block centered at ~1624.13 cm^{-1}. While comparing the FT-IR spectrum of LA conjugated with polymer, showed in scheme Step-2 strong absorption of the carbonyl band -O-C=O 1736.90 cm^{-1} was observed, confirming the peptide conjugation with polymer, amide carbonyl band -N-C=O 1646.11 cm^{-1} which thus provides evidence of ester bond and amide conformation in TTP-PEG_6-*b*-P (NVCL-*co*-HEA-*g*-LA) as shown in Fig.S2 (**A-C**).

3.3. Preparation and characterization of polymeric nanoparticles (PNPs)

Previous studies demonstrated that combining it with nab-paclitaxel improves prognosis modestly, yet it increases treatment-emergent toxicities [44]. The FOLFIRINOX regimen showed a survival improvement compared to single-agent Gem, but it also led to considerable toxicities [45]. Researchers are studying nanoparticles to deliver drug combinations with minimal side effects. However, the lack of a targeted delivery approach limits successful application. To address this, modified regimens and targeted therapies are being identified to optimize treatment outcomes using polymer nanotechnology [46]. However, the

Table 1
Hydrodynamic diameter, polydispersity index (PDI), and zeta potentials of respective polymer nanoparticles.

Formulation Name	Hydrodynamic diameter (nm)[a]	Polydispersity index (PDI)	Zeta Potentials (mV)
Empty Polymer (PNPs)	118. 08 ± 1.06	0.110 ± 0.010	+17.3 ± 2.06
P(Gem)	131.16 ± 0.89	0.175 ± 0.007	+22.1 ± 1.16
P(PTX)	140.51 ± 0.72	0.180 ± 0.09	+26.7 ± 3.06
P(Gem + PTX)	159. 82 ± 1.52	0.201 ± 0.012	+30.2 ± 2.2

[a] Measured by dynamic light scattering particle sizer.

Table 2
Total polymer weight, initial drug amount added, drug-loading efficiency (DLE), and encapsulation efficiency (EE) of single or dual drug-loaded polymer formulations.

Formulation Name	Total Polymer (mg/mL)	Initial drug added. (mg/mL)		DLE (%)[a]	EE (%)[b]
		Gem	PTX		
Polymer (P)	10.0	–	–	–	–
P(Gem)	10.0	2	–	3.9 ± 0.1	20.2 ± 1
P(PTX)	10.0	–	1	7.5 ± 0.2	81.5 ± 2
P(Gem + PTX)	10.0	2	1	4.2 ± 0.1 (Gem) 7.6 ± 0.3 (PTX)	22 ± 1 (Gem) 82.1 ± 0.3 (PTX)

[a] DLE = drug loading efficiency.
[b] EE = encapsulation efficiency.

tumor-targeted polymer formulations, which contained either a single or dual drug encapsulation, were prepared using a modified nano-precipitation method as described in the methods section. The empty and drug-loaded polymer formulations were analyzed for their hydrodynamic diameters, zeta potentials, and morphology using DLS and TEM techniques. Fig. 2A-H shows the average hydrodynamic diameters (Intensity %) and the morphology of PNPs. These include empty polymer nanoparticles (P) −118. 08 ± 1.06 nm (Fig. 2A), single drug-loaded polymer nanoparticles such as P(Gem)-131.16 ± 0.89 nm (Fig. 2B) and P(PTX)-140.51 ± 0.72 nm (Fig. 2C), and dual drug-loaded polymer nanoparticles P(Gem + PTX)-159. 82 ± 1.52 nm (Fig. 2D). All the PNPs have a narrow range of PDI from 0.11 to 0.21 and zeta potentials ranging from +17.3 ± 2.06 mV to +30. 2 ± 2.2 mV. The uniform spherical morphology of empty polymer (P) and single and dual drug-loaded PNPs (~50 nm) was observed in transmission electron micrographs (Fig. 2E–H). PNPs can potentially avoid fast systemic/renal clearance, facilitating efficient distribution in the targeted tumor sites through the enhanced permeability and retention effect [47]. All physicochemical characteristics, such as size, zeta potentials, and PDI values of the respective drug loaded TTP-polymer formulations, were compiled, and presented in Table 1.

To be a promising drug delivery vehicle, stability in the medium is crucial. The stability of empty PNPs and P(Gem + PTX) in deionized water was measured using the DLS technique (Fig. 2I). Hydrodynamic diameters of empty and drug-loaded PNPs showed no significant changes. Moreover, the selected drug encapsulation did not influence the polymer nano formulation's hydrodynamic diameter, PDI, and zeta potentials.

3.4. Drug loading and encapsulation efficiency

The study focused on the development of tumor-targeted polymer

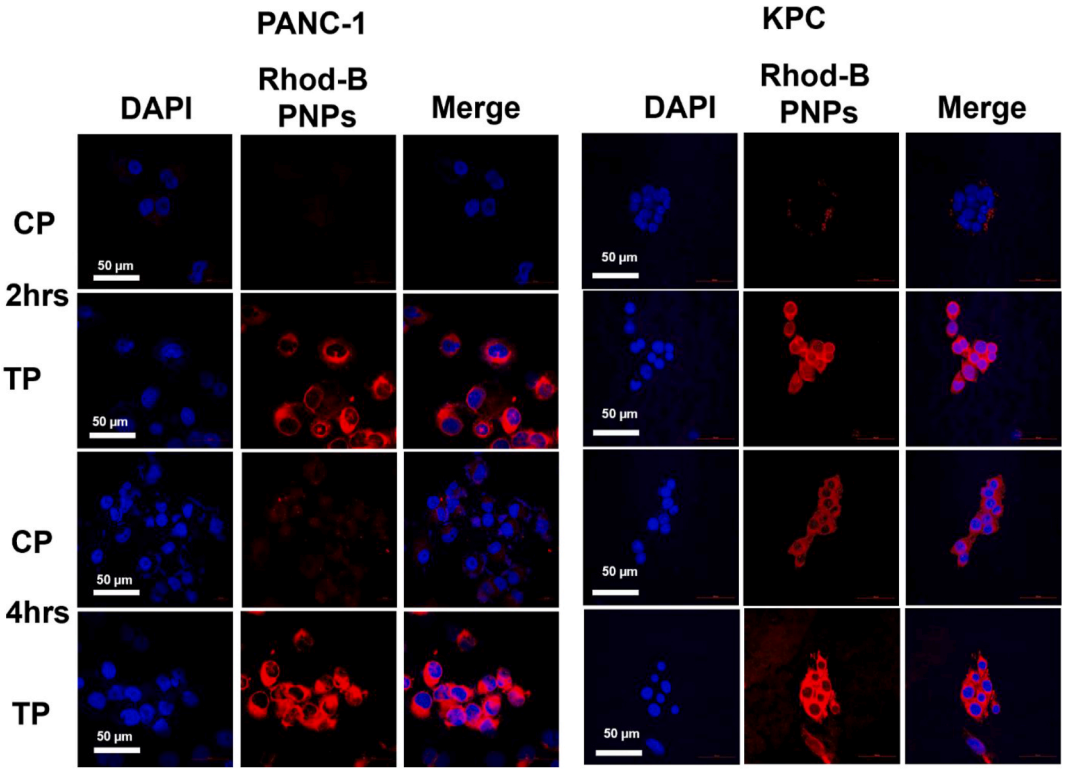

Fig. 3. *In vitro*, cellular uptake of Rhodamine-b labeled PNPs in cell lines. PANC-1 and KPC cells were treated with rhodamine-b loaded control polymer (CP) or TTP-conjugated polymer (TP) at two different time points: 2 h and 4 h. Nuclei are blue (DAPI), and rhodamine-b PNPs are red. Images were captured by confocal fluorescence microscopy under blue and red channels. TP-treated cells showed significantly higher uptake of rhodamine-B for both time points than CP-treated cells in two cell lines. Bar Length = 50 μm.

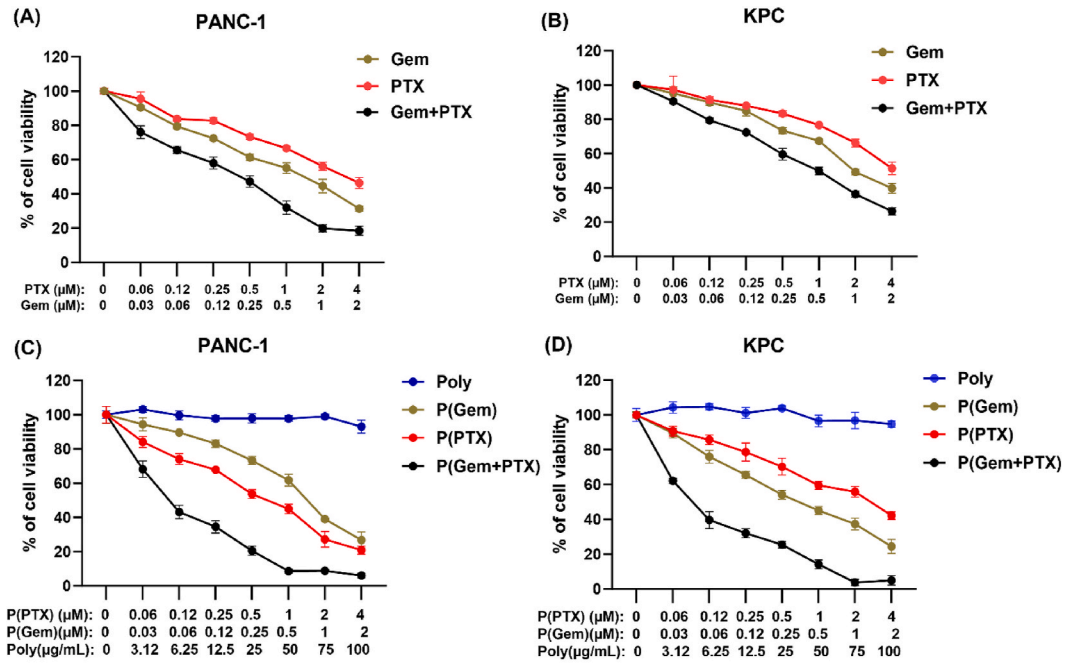

(E)

Group	PANC-1		KPC	
	IC_{50} (μM) ± SD	Combination Index(CI)	IC_{50} (μM) ± SD	Combination Index(CI)
Gem	0.777 ± 0.241	-	1.073 ± 0.073	-
PTX	3.293 ± 0.299	-	3.981 ± 0.183	-
Gem+PTX	0.185 ± 0.018 (Gem) 0.374 ± 0.036 (PTX)	0.25(Gem) 0.51(PTX)	0.417 ± 0.035 (Gem) 0.845 ± 0.069 (PTX)	0.50(Gem) 1.01(PTX)
P(Gem)	0.708 ± 0.035	-	0.264 ± 0.025	-
P(PTX)	0.575 ± 0.041	-	2.719 ± 0.280	-
P(Gem+PTX)	0.085 ± 0.003 (Gem) 0.173+0.006 (PTX)	0.24(Gem) 0.53(PTX)	0.084 ± 0.006 (Gem) 0.171 ± 0.011 (PTX)	0.34(Gem) 0.69(PTX)

Fig. 4. *In vitro* cellular cytotoxicity of empty or single and dual drug-loaded polymeric nanoparticles in combination with standard chemotherapeutic drugs gemcitabine and Paclitaxel in PDAC cell lines. PANC-1(left panel) and KPC (right panel). Cells were treated with indicated groups with varying concentrations for 72 h. **(A)**&**(B)** without formulation Gem, PTX, and Gem + PTX (Upper panel) and empty polymer and with polymer formulation **(C)**&**(D)** P, P(Gem), P(PTX), and P(Gem + PTX) (lower panel. Then, cell viability was determined by MTS assay. Each data point represents the quadruplet results obtained from a single experiment. **(E)** The table summarizes free drugs IC_{50} and combination Index values and their combinations and single and dual drug-loaded polymer nanoparticles.

formulations containing single or dual drug encapsulation. These formulations were prepared using a modified nanoprecipitation method outlined in the methods section. Table 2 summarizes of the amounts of polymer and drug used to formulate PNPs that either contained a single drug or two drugs. In addition, it shows their DLE and EE values. Lipophilic drugs, such as paclitaxel, had an EE of 81.5 %–82.1 % for both single- and dual-drug-loaded PNPs. However, the EE for the hydrophilic drug Gem was less than 25 % for both types of PNPs. This indicates that hydrophobic drugs had a higher EE compared to hydrophilic drugs. Both single- and dual-drug-loaded PNPs had a DLE of less than 8 %–10 %. There were no significant variations were observed among them in terms of EE and DLE, consistent with previous data published by several groups [17,48]. These formulations demonstrated excellent stability under *in vitro* physiological conditions.

3.5. *In vitro* drug release

The study assessed the impact of GSH on the release of Gem and PTX from TTP-PNPs at pH 7.4 and 37 °C. Fig. 2J illustrates that the release behavior is dependent on the presence of GSH. GSH concentrations

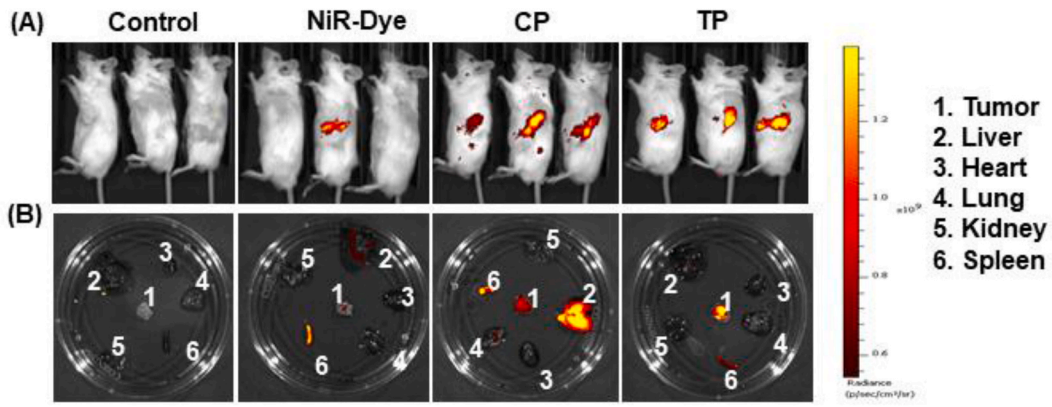

Fig. 5. Biodistribution of tumor-targeted peptide polymer nanoparticles (PNPs) in an orthotopic PDAC model. **(A)** Different combinations of PNPs, including control - no treatment: NiR dye formulation; CP: Polymer formulation without TTP; TP with TTP, were injected, and IVIS images were at 24 h. **(B)** Ex vivo imaging of the tumors and major organs was isolated and examined after 24 h.

(~2–10 mM) inside cancer cells are significantly higher (2–10 mM) compared to the extracellular environment (typically 1–10 μM). This difference in GSH concentrations plays a crucial role in the controlled release of drugs from the TTP-PNPs, a key finding of this study [49]. Notably, in 24 h at 37 °C and pH 7.4, less than 20 % of the Gem and 15 % PTX were released from P(Gem + PTX), a highly stable in blood circulation. However, the release of both Gem and PTX from the PNPs increased to more than 85 % and 90 %, respectively, when the GSH concentration was 10 mM. These findings PNPs take up the tumor cells, glutathione concentrations within the cancer cells trigger the S–S bond LA and, additionally, mild hyperthermia externally, taking advantage of their N-Vinyl caprolactam group's thermo-responsive behavior, which helps disturb the complete nanoformulation and releases the of the encapsulated GEM and PTX and as shown in graphical abstract. It suggest that P(Gem + PTX) may be stable in circulation while quickly releasing drugs after entering the cell [38].

3.6. *In vitro cellular uptake of Rhodamine-B loaded polymer nanoparticles in PDAC cell lines*

We conducted *in vitro* cellular uptake studies using Rhodamine-B-loaded polymer formulation at two different time points (2 h, 4 h) to assess the efficacy of our newly developed targeted PNPs. As shown in Fig. 3, cellular uptake was significantly higher at both time points for the TTP-PNPs (TP) in both KPC and PANC-1 Cell lines. In contrast, minimal cellular uptake was observed for the PNPs without TTP (CP). These results suggest the higher targeting efficiency of TTP-PNPs.

3.7. *In vitro cytotoxicity of dual drug-loaded TTP-PNPs in PDAC cells*

Following promising cellular uptake, we investigated the cytotoxic effects of the polymer nanocarrier system on PANC-1 and KPC cells when delivering single or combined drugs. We analyzed the impact of different concentrations of free drugs and their combination, as well as PNPs, single and dual drug-loaded PNPs such as P(Gem), P(PTX), and P (Gem + PTX) on the two cell lines using the MTS assay. We used GraphPad Prism software to calculate the IC_{50} value of each drug and the combination index (CI) of combination chemotherapy [50]. Gem/PTX combinations with various concentrations of Gem and PTX keeping their molar ratio 1:2 (i.e. 2:4, 1:2, 0.5:1, 0.25:0.5, 0.125: 0.25, 0.06: 0.125 and 0.03:0.06) was used in this experiment. The cytotoxicity demonstrated concentration-dependency in all treatment groups after 72 h. The combination of Gem and PTX proved more effective against PANC-1 and KPC cancer cells than the individual drugs, as shown in Fig. 4 A and 4B. The IC_{50} values of the Gem + PTX combination were lower than those of individual drugs. For PANC-1 cells, the IC_{50} values were 0.185 ± 0.018 for Gem + PTX and 0.777 ± 0.241 for free Gem alone. For KPC cells, the IC_{50} values were 0.417 ± 0.035 for Gem + PTX and 1.037 ± 0.073 for free Gem alone. Similarly, for PANC-1 cells, the IC_{50} values were 0.374 ± 0.035 for Gem + PTX and 3.293 ± 0.299 for free PTX alone. For KPC cells, the IC_{50} values were 0.845 ± 0.069 for Gem + PTX and 3.981 ± 0.183 for free PTX alone, as shown in Fig. 4E. The CI of the Gem + PTX was less than 1 in PANC-1 and less than or equal to 1 in KPC cells, indicating a moderate synergistic effect between Gem and PTX. Fig. 4C and 4D show single and dual-loaded PNPs and PNPs. PNPs did not cause any significant cytotoxicity at concentrations up to 100 μg/mL, which was higher than the maximum concentrations used in the drug-loading PNPs. P(Gem + PTX) had considerably lowered IC_{50} (μM) of 0.085 ± 0.003/0.084 ± 0.006 with respect to Gem and 0.173 ± 0.006/0.171 ± 0.011 with respect to PTX in PANC-1/KPC cell lines compared to IC_{50} (μM) of P(Gem) and P(PTX) as shown in Fig. 4E. The IC_{50} of P(Gem + PTX) was 2.4-fold lower in PANC-1 and 5.2-fold lower in KPC cells compared to free Gem + PTX in both cell lines. The CI of Gem and PTX in dual drug-loaded PNPs such as P(Gem + PTX) were 0.24 and 0.34 with respect to Gem and 0.53 and 0.69 with respect to PTX in PANC-1 and KPC cell lines respectively, it was pointing to a strong synergistic effect between Gem and PTX in P(Gem + PTX) treated cells. Combination chemotherapy has been linked to reduced systemic toxicity when it shows synergistic effects [51]. We then conducted a cytotoxicity study to compare the effects of P(Gem + PTX) on PANC-1 cells with those on two types of noncancer cell lines: HUVEC and HPDECs. The noncancer lines showed no toxicity even at high concentrations. However, we observed toxicity in PANC-1 cell lines when using PTX: Gem ratios ranging from 0.25:0.12 μM to 4:2 μM, as shown in Fig. S3. The results from the MTS assay indicated that P(Gem + PTX) demonstrated better cytotoxicity than all control groups, such as pristine drugs and their combinations, and single drug-loaded PNPs in both KPC and PANC-1 cell lines, as well as no toxicity observed in normal cells, indicated that TTP-PNPs formulation more targeting and systematic release efficiency.

3.8. *In vivo tumor biodistribution of NiR dye-loaded TTP-PNPs in PDAC xenografts*

We further investigated the efficacy of our newly developed TTP-PNPs for targeting tumors *in vivo*. To prevent the usual interference of tissue autofluorescence signal associated with Rhodamine-B, we employed NiR dye-loaded PNPs instead. NiR dye absorbs and emits in the IR region of the spectrum, which is less absorbed by living tissue, therefore resulting in minimal autofluorescence that could interfere with the actual signal intensity. We injected NiR-dye labeled TTP- PNPs (TP) and PNPs without TTP (CP) and NiR dye solution via the i.v route in

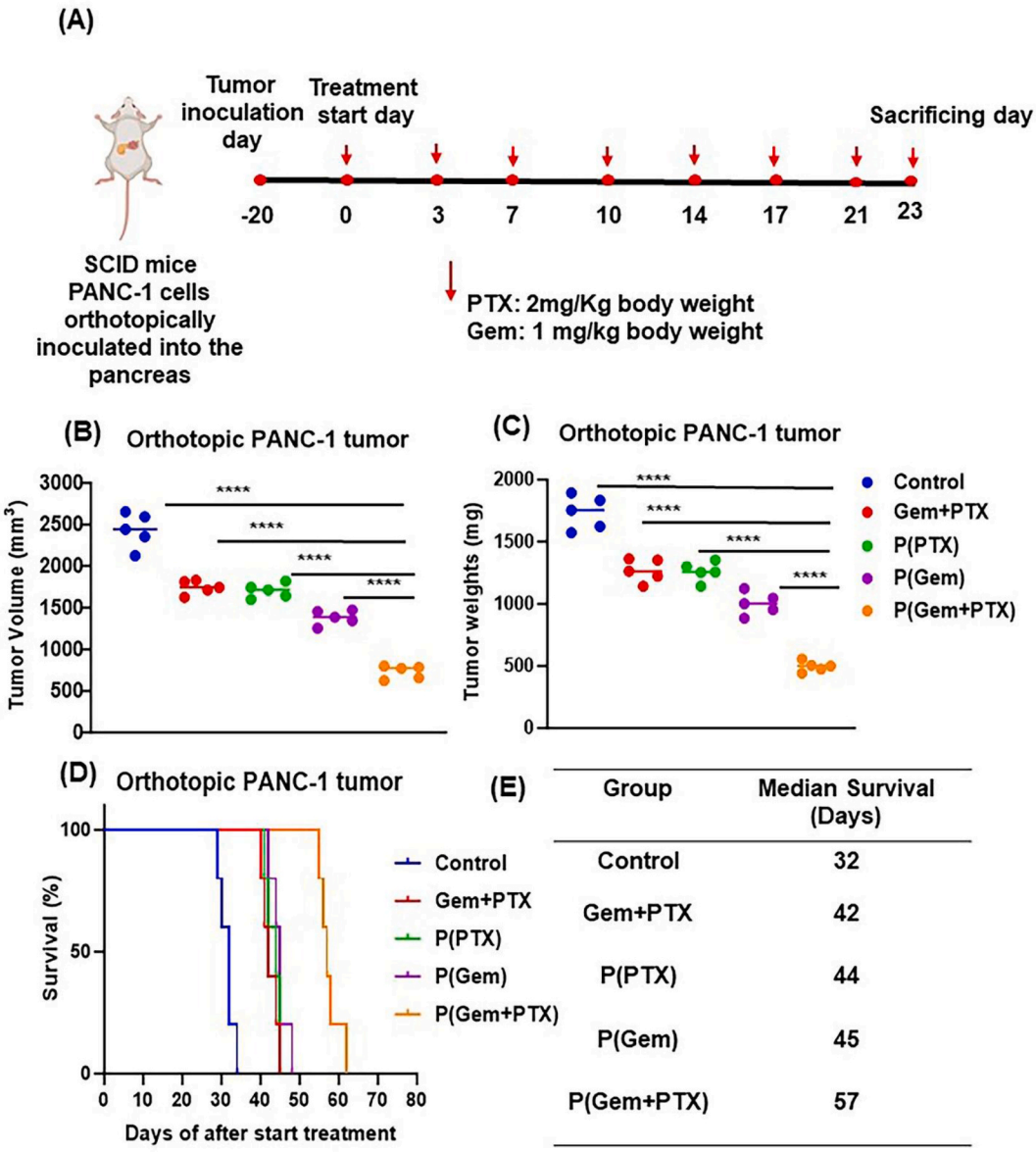

Fig. 6. Anti-tumor and survival effects of combination of TTP-polymeric loaded paclitaxel and Gemcitabine treatments in pancreatic orthotopic mouse model: Mice bearing PANC-1 orthotopic pancreatic tumors were divided into five treatment groups (n = 5) control (PNPs), pristine (PTX + Gem), P(Gem), P(PTX) and P(PTX + Gem). The PNPs group was used as a control. **(A)** experimental plan, **(B)** tumor volume, **(C)** tumor weight and **(D)** survival curves in PANC-1 orthotopic pancreatic tumor-bearing mice treated as above (n = 5) **(E)** survival of each group in days. Throughout the experiment, we used paclitaxel 2 mg/kg and gemcitabine 1 mg/kg **** denotes $p < 0.0001$ compared to the indicated respective group.

mice bearing orthotopic PANC-1 xenografts. As shown in Fig. 5A, the TP showed a higher tumor-specific signal than the CP and NiR dye groups at 24 h after i.v injection. Furthermore, the ex vivo imaging of the tumors and significant organs also confirmed that TP had a higher tumor-specific signal than CP (Fig. 5B). TP formulation shows less dye accumulation in the liver than the other groups, suggesting less hepatotoxicity. The findings summarized in Fig. 5 are consistent with the notion that our newly developed TTP-PNPs efficiently deliver anticancer drugs selectively to tumors. These results provide strong evidence that the novel TTP-PNPs, aimed at targeting tumors, are efficient and safe for delivering anticancer agents directly to tumors.

3.9. *In vivo efficacy of drug-loaded PNPs in PDAC tumor models*

Nel's group showed that PTX/Gem-loaded LB-MSN at doses of 100 mg/kg and 10 mg/kg per injection had a synergistic effect in inhibiting tumor growth in PC compared to only Gem-loaded LB-MSN or gem plus Abraxane [52]. Kokkali and colleagues discovered that targeted nanoparticles in hydrogel can effectively deliver Gem and PTX to PC, inhibiting PANC-1 growth significantly [53]. Another study found that Gem plus PTX-loaded liposomes significantly induced apoptosis compared to Gem-loaded liposomes in PC cells *in vitro* [54]. Researchers recently developed Gem and PTX coloaded nanoparticles, including liposomes and PLGA nanoparticles, for selective cancer therapy [48]. However, although not part of the standard chemotherapy regimen, polymeric nanoparticles, and micelles have been utilized to administer cisplatin, doxorubicin, and camptothecin to explore alternative treatments for PDAC [55]. The recently published review article discussed several other combinations of drug-based nanoparticle treatments and Gem [6].

This study aimed to assess the effectiveness of drug-loaded polymer nanoparticles in PANC-1 xenografts and the syngeneic KPC model, the efficacy of P(Gem + PTX) in PANC-1 xenografts, and the results are summarized in Fig. 6. Fig. 6A describes our *in vivo* experimental plan for

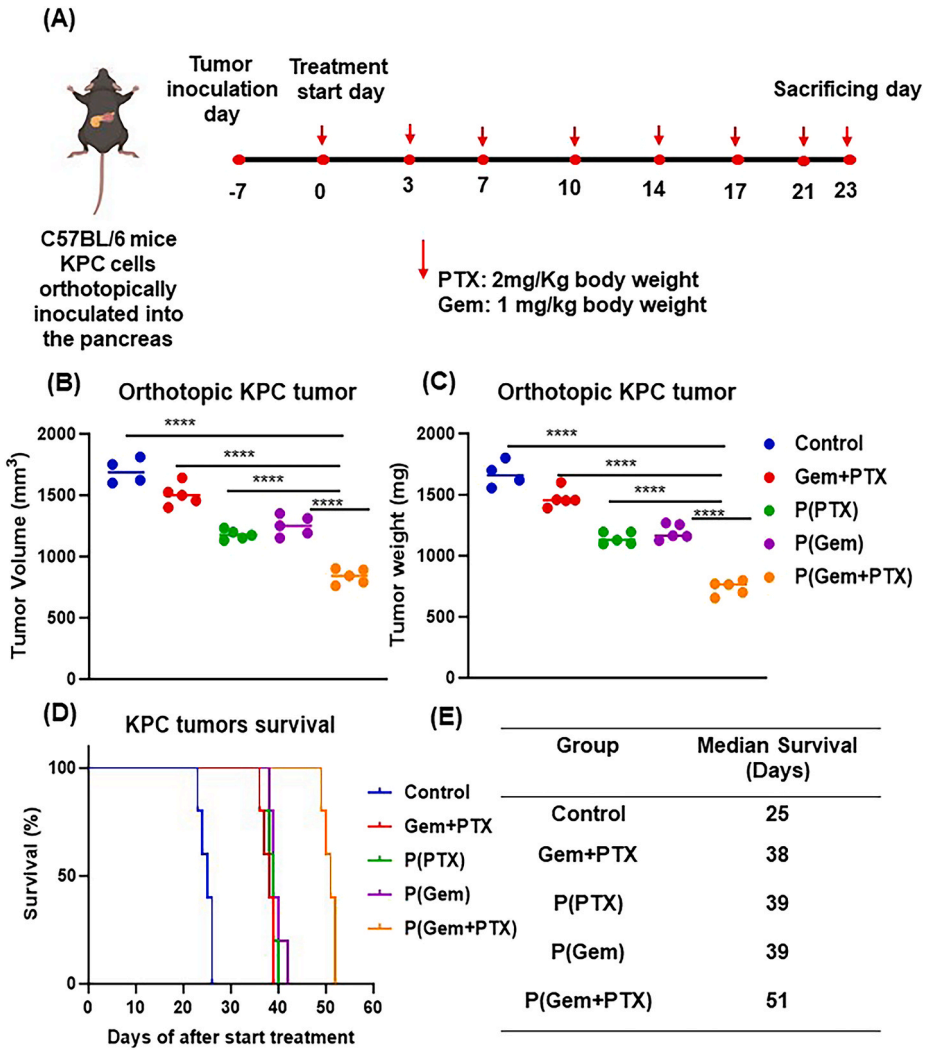

Fig. 7. Anti-tumor and survival effects of combination of TTP-polymeric loaded paclitaxel and Gemcitabine treatments in pancreatic orthotopic mouse model: Mice bearing KPC orthotopic pancreatic tumors were treated with five deafferentations (n = 5) Control, Pristine (PTX + Gem), P(Gem), P (PTX) and P(PTX + Gem). The PNP group was used as a control. **(A)** experimental plan, **(B)** tumor volume, **(C)** tumor weight, and **(D)** survival curves KPC orthotopic pancreatic tumor-bearing mice treated as above (n = 5) **(E)** survival of each group in days. had a higher survival rate than individual drug treatments or control mice. Throughout the experiment, we used paclitaxel 2 mg/kg and gemcitabine 1 mg/kg **** denotes $p < 0.0001$ compared to the indicated respective group.

the tumor growth inhibition study, Fig. 6B shows tumor volume, and Fig. 6C shows tumor weight, respectively. We administered drugs with the concentration of 2 mg/kg PTX and 1 mg/kg Gem twice a week for three weeks via the i.v route. These doses were significantly lower than those mentioned in previous studies [56]. Tumor volumes in P(Gem + PTX) treated group (727 ± 30 mm^3) were significantly smaller in comparison with Control (2433.2 ± 209.7 mm^3) or P(Gem) (1382 ± 88.09 mm^3) or P(PTX) (1383 ± 86.09 mm^3) and free Gem + PTX (1744.6 ± 83.0 mm^3) groups (Fig. 6B). The results obtained from the tumor weights measurements also showed similar patterns in (Fig. 6C). Body weight of the P(Gem + PTX) treated group shows no weight loss, while the control groups exhibited drastic body weight reduction shown in Fig. S4A. Another set of experiments was conducted to estimate different treatment groups' median survival. A similar *in vivo* experimental plan (Fig. 6A) was used for the survival study. The group that received P(Gem + PTX) treatment had a notably higher median survival rate of 57 days compared to the control group (32 days), as well as the groups that received either P(Gem) (45 days), P(PTX) (44 days), or Gem + PTX (42 days), as illustrated in Fig. 6D and summarized in Fig. 6E.

To test whether this observed effect of P(Gem + PTX) holds in another pancreatic tumor model, we repeated the tumor growth inhibition and survival studies in a syngeneic KPC model developed in C57BL6, shown in Fig. 7A-E. Here, we administered the same drug concentrations as the PANC-1 tumor. Similar patterns of results were observed in this model. The combination therapy decreased tumor volume and weight and showed no loss in the body weights compared to the control groups (Fig. 7B&C and Fig. S4B). We also observed a significant improvement in survival in the P(Gem + PTX) group compared to other treatment groups (Fig. 7D-E).

Further, the PANC-1 and KPC tumor sections were stained with hematoxylin and eosin (H&E) to analyze the tumor growth (Fig. 8A, first and third row). Fewer nuclei staining in P(Gem + PTX) treatment group tumor sections than P(Gem), P(PTX), and (Gem + PTX) indicates that there has been more tumor necrosis because of the dual drug treatment. The tumor sections were subjected to Ki67 staining to examine the proliferation state of the tumors, as shown in (Fig. 8A, second and fourth row). P(Gem + PTX) showed less Ki67 staining compared to other controls. Additionally, the quantification results for Ki67-positive nuclei (Fig. 8B) corroborated with H & E. Our study's findings suggest that polymer nanoformulations can offer a more effective treatment option, as the mice treated with these nanoformulations showed healthier outcomes compared to the control, we conducted histological analysis of

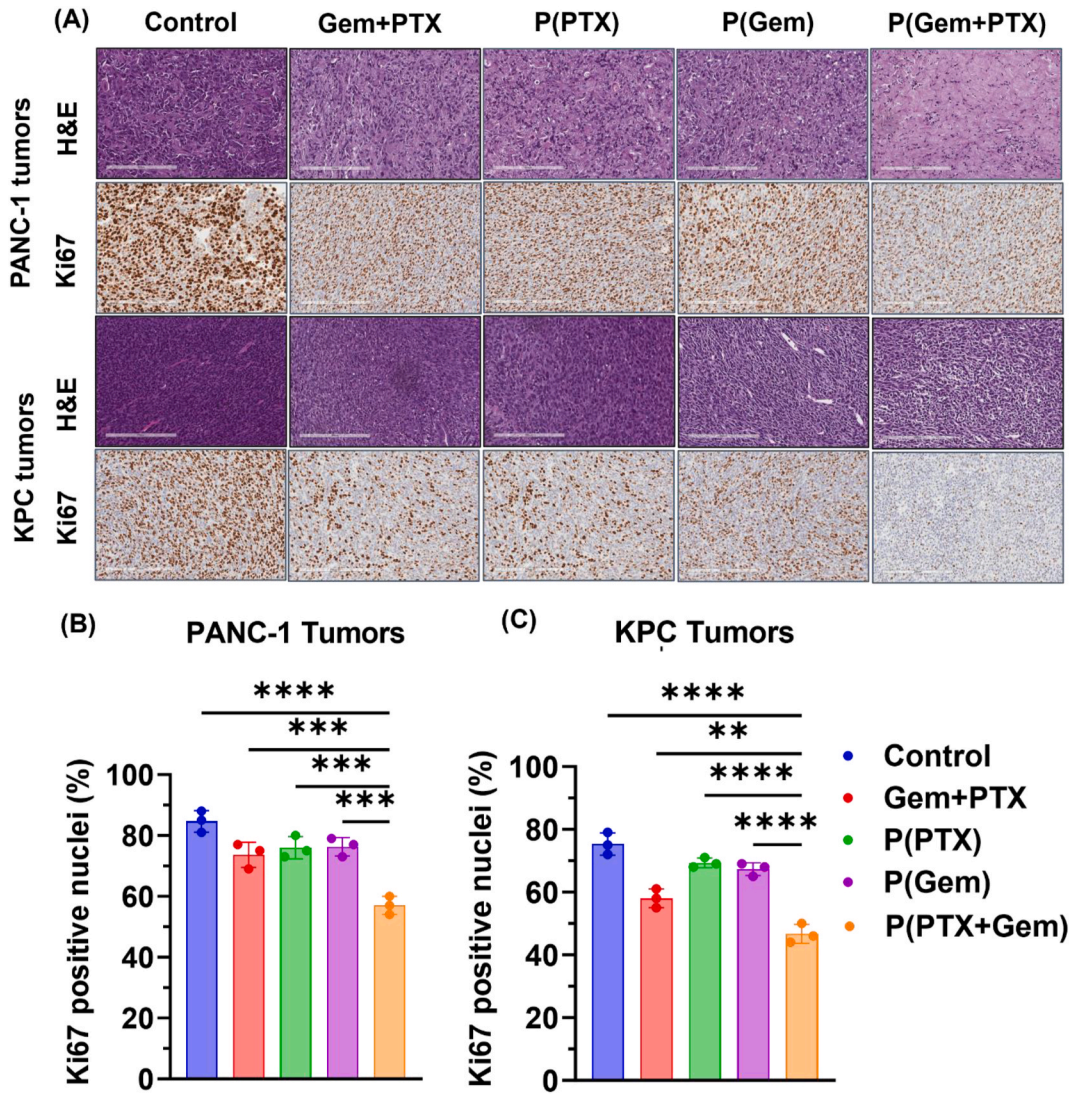

Fig. 8. H&E and Ki67 staining of tumor sections. (A). Representative images of the H&E-stained tumor sections from different treatment groups displayed comparatively higher anti-proliferative activity of P(Gem + PTX). **(B)&(C)** Quantification of Ki67 positive nuclei in PANC-1 and KPC tumor sections * and *** denotes $p < 0.05$ and $p < 0.001$ compared to untreated, respectively.

major organs to confirm the non-toxicity of P(Gem + PTX) nanoformulation and found no pathological changes in histological specimens of the P(Gem + PTX) group. The lung, heart, kidney, spleen, and liver tissue sections analyzed using H&E staining showed no signs of fibrosis, inflammation, or abnormal structures, as shown in Fig. S5. These results indicate that our nanoformulations are safe for major organs and can be a promising approach to cancer treatment.

4. Conclusion

We have developed a nano-delivery system using a multi-functional tumor-targeting polymer nanocarrier that can simultaneously deliver a hydrophilic chemotherapeutic drug (GEM) and a hydrophobic drug (PTX) for treating PDAC. These TTP-PNPs have shown significant stability, drug release, and the ability to target and eliminate pancreatic cancer cells selectively. By delivering Gem and PTX together in TTP-PNPs, we can maximize the therapeutic benefits of this synergistic drug combination while potentially reducing toxic side effects. targeted polymer nanoparticles could be an effective drug delivery system for PDAC treatment. These findings collectively underscore the promising potential of the developed tumor-targeting polymer nanocarrier as an effective drug delivery system for PDAC therapy. The study's comprehensive approach, from synthesis to *in vivo* efficacy, provides valuable insights into the design and application of advanced polymeric nanocarriers for targeted and efficient cancer treatment. These results suggest that TTP-PNPs are very promising for future clinical treatment of PDAC and open an avenue for further exploration and development of such nanocarriers in cancer therapeutics.

Funding

This work was supported by National Institute of Health (NIH) grants CA78383 (DM). National Institute of Health (NIH) grants CA150190 (DM). The National Heart, Lung, and Blood Institute (NHLBI) grants HL 140411 (DM). Florida Department of Health grant 91803004 (DM). Department of Defence (DoD) Early Career Investigator award W81XWH-21-1-0678 (KP).

Data and materials availability

All necessary data to evaluate the paper's conclusions are available in the paper and Supplementary Materials.

CRediT authorship contribution statement

Naga Malleswara Rao Nakka: Writing – original draft, Visualization, Validation, Methodology, Investigation, Formal analysis, Data curation. **Hari Krishnareddy Rachamala:** Validation, Methodology, Data curation. **Ramcharan Singh Angom:** Methodology. **Nagamalleswara Rao Indla:** Data curation. **Shamit Kumar Dutta:** Methodology. **Enfeng Wang:** Methodology. **Santanu Bhattacharya:** Writing – review & editing, Methodology. **Annadanam V. Sesha Sainath:** Writing – review & editing. **Hani Babiker:** Writing – review & editing. **Krishnendu Pal:** Writing – review & editing, Writing – original draft, Supervision, Data curation. **Debabrata Mukhopadhyay:** Writing – review & editing, Supervision, Project administration, Funding acquisition, Conceptualization.

Declaration of competing interest

The authors declare the following financial interests/personal relationships which may be considered as potential competing interests: Debabrata Mukhopadhyay has patent pending to Debabrata Mukhopadhyay. If there are other authors, they declare that they have no known competing financial interests or personal relationships that could have appeared to influence the work reported in this paper.

Data availability

Data will be made available on request.

Acknowledgement

The authors would like to thank Brandy Edenfield for immunohistochemistry and Laura Lewis-Tuffin for assisting with digitizing the slides. The authors also thank the Mayo Clinic Microscopy and Cell Analysis Core for experimental and technical support.

Appendix A. Supplementary data

Supplementary data to this article can be found online at https://doi.org/10.1016/j.mtbio.2024.101199.

References

[1] Cancer Stat Facts: Pancreatic Cancer, 5-Year Relative Survival, 2024. https://seer.cancer.gov/statfacts/html/pancreas.html. (Accessed 1 January 2024).
[2] A.L. Blackford, M.I. Canto, A.P. Klein, R.H. Hruban, M. Goggins, Recent trends in the incidence and survival of stage 1A pancreatic cancer: a surveillance, epidemiology, and end results analysis, J. Natl. Cancer Inst. 112 (11) (2020) 1162–1169.
[3] A. Adamska, A. Domenichini, M. Falasca, Pancreatic ductal adenocarcinoma: current and evolving therapies, Int. J. Mol. Sci. 18 (7) (2017).
[4] P. Hammel, F. Huguet, J.L. van Laethem, D. Goldstein, B. Glimelius, P. Artru, I. Borbath, O. Bouché, J. Shannon, T. André, L. Mineur, B. Chibaudel, F. Bonnetain, C. Louvet, Effect of chemoradiotherapy vs chemotherapy on survival in patients with locally advanced pancreatic cancer controlled after 4 Months of gemcitabine with or without erlotinib: the LAP07 randomized clinical trial, JAMA 315 (17) (2016) 1844–1853.
[5] I. Garrido-Laguna, M. Hidalgo, Pancreatic cancer: from state-of-the-art treatments to promising novel therapies, Nat. Rev. Clin. Oncol. 12 (6) (2015) 319–334.
[6] K. Samanta, S. Setua, S. Kumari, M. Jaggi, M.M. Yallapu, S.C. Chauhan, Gemcitabine combination nano therapies for pancreatic cancer, Pharmaceutics 11 (11) (2019).
[7] M.J. Moore, D. Goldstein, J. Hamm, A. Figer, J.R. Hecht, S. Gallinger, H.J. Au, P. Murawa, D. Walde, R.A. Wolff, D. Campos, R. Lim, K. Ding, G. Clark, T. Voskoglou-Nomikos, M. Ptasynski, W. Parulekar, Erlotinib plus gemcitabine compared with gemcitabine alone in patients with advanced pancreatic cancer: a phase III trial of the National Cancer Institute of Canada Clinical Trials Group, J. Clin. Oncol. 25 (15) (2007) 1960–1966.
[8] Q.Y. Meng, H.L. Cong, H. Hu, F.J. Xu, Rational design and latest advances of codelivery systems for cancer therapy, Mater Today Bio 7 (2020) 100056.
[9] S.F. Jones, J.R. Infante, D.R. Spigel, N.W. Peacock, D.S. Thompson, F.A. Greco, W. McCulloch, H.A. Burris, 3rd, Phase 1 results from a study of romidepsin in combination with gemcitabine in patients with advanced solid tumors, Cancer Invest. 30 (6) (2012) 481–486.
[10] C. Sun, D. Ansari, R. Andersson, D.Q. Wu, Does gemcitabine-based combination therapy improve the prognosis of unresectable pancreatic cancer? World J. Gastroenterol. 18 (35) (2012) 4944–4958.
[11] K.K. Frese, A. Neesse, N. Cook, T.E. Bapiro, M.P. Lolkema, D.I. Jodrell, D. A. Tuveson, nab-Paclitaxel potentiates gemcitabine activity by reducing cytidine deaminase levels in a mouse model of pancreatic cancer, Cancer Discov. 2 (3) (2012) 260–269.
[12] D.D. Von Hoff, T. Ervin, F.P. Arena, E.G. Chiorean, J. Infante, M. Moore, T. Seay, S. A. Tjulandin, W.W. Ma, M.N. Saleh, M. Harris, M. Reni, S. Dowden, D. Laheru, N. Bahary, R.K. Ramanathan, J. Tabernero, M. Hidalgo, D. Goldstein, E. Van Cutsem, X. Wei, J. Iglesias, M.F. Renschler, Increased survival in pancreatic cancer with nab-paclitaxel plus gemcitabine, N. Engl. J. Med. 369 (18) (2013) 1691–1703.
[13] V. Heinemann, M. Reni, M. Ychou, D.J. Richel, T. Macarulla, M. Ducreux, Tumour-stroma interactions in pancreatic ductal adenocarcinoma: rationale and current evidence for new therapeutic strategies, Cancer Treat Rev. 40 (1) (2014) 118–128.
[14] Z. Edis, J. Wang, M.K. Waqas, M. Ijaz, M. Ijaz, Nanocarriers-Mediated drug delivery systems for anticancer agents: an overview and perspectives, Int. J. Nanomed. 16 (2021) 1313–1330.
[15] S.N. Moya Betancourt, J.G. Uranga, V.B. Daboin, P.G. Bercoff, J.S. Riva, Chapter 9 - metallic nanoparticles-based drug delivery for pancreatic cancer, in: P. Kesharwani, N. Gupta (Eds.), Recent Advances in Nanocarriers for Pancreatic Cancer Therapy, Academic Press, 2024, pp. 213–237.
[16] E.K. Silli, M. Li, Y. Shao, Y. Zhang, G. Hou, J. Du, J. Liang, Y. Wang, Liposomal nanostructures for Gemcitabine and Paclitaxel delivery in pancreatic cancer, Eur. J. Pharm. Biopharm. 192 (2023) 13–24.
[17] X. Jiang, M.J. Lee, T. Luo, L. Tillman, W. Lin, Co-delivery of three synergistic chemotherapeutics in a core-shell nanoscale coordination polymer for the treatment of pancreatic cancer, Biomaterials 301 (2023) 122235.
[18] C.R. Patra, R. Bhattacharya, E. Wang, A. Katarya, J.S. Lau, S. Dutta, M. Muders, S. Wang, S.A. Buhrow, S.L. Safgren, M.J. Yaszemski, J.M. Reid, M.M. Ames, P. Mukherjee, D. Mukhopadhyay, Targeted delivery of gemcitabine to pancreatic adenocarcinoma using cetuximab as a targeting agent, Cancer Res. 68 (6) (2008) 1970–1978.
[19] J.A. Khan, R.A. Kudgus, A. Szabolcs, S. Dutta, E. Wang, S. Cao, G.L. Curran, V. Shah, S. Curley, D. Mukhopadhyay, J.D. Robertson, R. Bhattacharya, P. Mukherjee, Designing nanoconjugates to effectively target pancreatic cancer cells in vitro and in vivo, PLoS One 6 (6) (2011) e20347.
[20] T. Kottke, N. Boisgerault, R.M. Diaz, O. Donnelly, D. Rommelfanger-Konkol, J. Pulido, J. Thompson, D. Mukhopadhyay, R. Kaspar, M. Coffey, H. Pandha, A. Melcher, K. Harrington, P. Selby, R. Vile, Detecting and targeting tumor relapse by its resistance to innate effectors at early recurrence, Nat. Med. 19 (12) (2013) 1625–1631.
[21] R.H. Prabhu, V.B. Patravale, M.D. Joshi, Polymeric nanoparticles for targeted treatment in oncology: current insights, Int. J. Nanomed. 10 (2015) 1001–1018.
[22] S. Naderinezhad, G. Amoabediny, F. Haghiralsadat, Co-delivery of hydrophilic and hydrophobic anticancer drugs using biocompatible pH-sensitive lipid-based nano-carriers for multidrug-resistant cancers, RSC Adv. 7 (48) (2017) 30008–30019.
[23] T. Skotland, T.G. Iversen, A. Llorente, K. Sandvig, Biodistribution, pharmacokinetics and excretion studies of intravenously injected nanoparticles and extracellular vesicles: possibilities and challenges, Adv. Drug Deliv. Rev. 186 (2022) 114326.
[24] U.S. Toti, B.R. Guru, A.E. Grill, J. Panyam, Interfacial activity assisted surface functionalization: a novel approach to incorporate maleimide functional groups and cRGD peptide on polymeric nanoparticles for targeted drug delivery, Mol. Pharm. 7 (4) (2010) 1108–1117.
[25] V. Sanna, N. Pala, M. Sechi, Targeted therapy using nanotechnology: focus on cancer, Int. J. Nanomed. 9 (2014) 467–483.
[26] X. Wu, H. Huang, C. Wang, S. Lin, Y. Huang, Y. Wang, G. Liang, Q. Yan, J. Xiao, J. Wu, Y. Yang, X. Li, Identification of a novel peptide that blocks basic fibroblast growth factor-mediated cell proliferation, Oncotarget 4 (10) (2013) 1819–1828.
[27] T.P. Thomas, R. Shukla, A. Kotlyar, J. Kukowska-Latallo, J.R. Baker Jr., Dendrimer-based tumor cell targeting of fibroblast growth factor-1, Bioorg. Med. Chem. Lett 20 (2) (2010) 700–703.
[28] N. Porębska, A. Knapik, M. Poźniak, M.A. Krzyścik, M. Zakrzewska, J. Otlewski, Ł. Opaliński, Intrinsically fluorescent oligomeric cytotoxic conjugates toxic for FGFR1-overproducing cancers, Biomacromolecules 22 (12) (2021) 5349–5362.
[29] V.S. Madamsetty, K. Pal, S.K. Dutta, E. Wang, D. Mukhopadhyay, Targeted dual intervention-oriented drug-encapsulated (DIODE) nanoformulations for improved treatment of pancreatic cancer, Cancers 12 (5) (2020).
[30] K. Pal, F. Al-Suraih, R. Gonzalez-Rodriguez, S.K. Dutta, E. Wang, H.S. Kwak, T. R. Caulfield, J.L. Coffer, S. Bhattacharya, Multifaceted peptide assisted one-pot synthesis of gold nanoparticles for plectin-1 targeted gemcitabine delivery in pancreatic cancer, Nanoscale 9 (40) (2017) 15622–15634.
[31] H.M. Kolbeinsson, S. Chandana, G.P. Wright, M. Chung, Pancreatic cancer: a review of current treatment and novel therapies, J. Invest. Surg. 36 (1) (2023) 2129884.
[32] U. Dristant, K. Mukherjee, S. Saha, D. Maity, An overview of polymeric nanoparticles-based drug delivery system in cancer treatment, Technol. Cancer Res. Treat. 22 (2023) 15330338231152083.
[33] K. Pal, V.S. Madamsetty, S.K. Dutta, D. Mukhopadhyay, Co-delivery of everolimus and vinorelbine via a tumor-targeted liposomal formulation inhibits tumor growth and metastasis in RCC, Int. J. Nanomed. 14 (2019) 5109–5123.
[34] L. Ahmadkhani, M. Abbasian, A. Akbarzadeh, Synthesis of sharply thermo and PH responsive PMA-b-PNIPAM-b-PEG-b-PNIPAM-b-PMA by RAFT radical polymerization and its schizophrenic micellization in aqueous solutions, Des. Monomers Polym. 20 (1) (2017) 406–418.

[35] D. Mukhopadhyay, V.S. Madamsetty, K. Pal, Drug Delivery Methods and Compositions, Google Patents, 2022.
[36] N.N.M. Rao, S. Sharma, K.K. Palodkar, V. Sadhu, M. Sharma, A.V.S. Sainath, Rationally designed curcumin laden glycopolymeric nanoparticles: implications on cellular uptake and anticancer efficacy, J. Appl. Polym. Sci. 137 (32) (2020).
[37] Y. Zou, J. Wei, Y. Xia, F. Meng, J. Yuan, Z. Zhong, Targeted chemotherapy for subcutaneous and orthotopic non-small cell lung tumors with cyclic RGD-functionalized and disulfide-crosslinked polymersomal doxorubicin, Signal Transduct. Targeted Ther. 3 (2018) 32.
[38] A. Kumar Sauraj, B. Kumar, A. Kulshreshtha, Y.S. Negi, Redox-sensitive nanoparticles based on xylan-lipoic acid conjugate for tumor targeted drug delivery of niclosamide in cancer therapy, Carbohydr. Res. 499 (2021) 108222.
[39] T. Kulkarni, D. Mukhopadhyay, S. Bhattacharya, Nanomechanical insight of pancreatic cancer cell membrane during receptor mediated endocytosis of targeted gold nanoparticles, ACS Appl. Bio Mater. 4 (1) (2021) 984–994.
[40] W. Guo, Y. Song, W. Song, Y. Liu, Z. Liu, D. Zhang, Z. Tang, O. Bai, Co-Delivery of doxorubicin and curcumin with polypeptide nanocarrier for synergistic lymphoma therapy, Sci. Rep. 10 (1) (2020) 7832.
[41] H.K. Rachamala, V.S. Madamsetty, R.S. Angom, N.M. Nakka, S.K. Dutta, E. Wang, D. Mukhopadhyay, K. Pal, Targeting mTOR and survivin concurrently potentiates radiation therapy in renal cell carcinoma by suppressing DNA damage repair and amplifying mitotic catastrophe, J. Exp. Clin. Cancer Res. 43 (1) (2024) 159.
[42] W. Qiu, G.H. Su, Development of orthotopic pancreatic tumor mouse models, Methods Mol. Biol. 980 (2013) 215–223.
[43] H. Uusi-Kerttula, M. Legut, J. Davies, R. Jones, E. Hudson, L. Hanna, R.J. Stanton, J.D. Chester, A.L. Parker, Incorporation of peptides targeting EGFR and FGFR1 into the adenoviral fiber knob domain and their evaluation as targeted cancer therapies, Hum. Gene Ther. 26 (5) (2015) 320–329.
[44] S.K. Hsu, M. Jadhao, W.T. Liao, W.T. Chang, C.T. Hung, C.C. Chiu, Culprits of PDAC resistance to gemcitabine and immune checkpoint inhibitor: tumour microenvironment components, Front. Mol. Biosci. 9 (2022) 1020888.
[45] T. Conroy, F. Desseigne, M. Ychou, O. Bouché, R. Guimbaud, Y. Bécouarn, A. Adenis, J.-L. Raoul, S. Gourgou-Bourgade, C. de la Fouchardière, J. Bennouna, J.-B. Bachet, F. Khemissa-Akouz, D. Péré-Vergé, C. Delbaldo, E. Assenat, B. Chauffert, P. Michel, C. Montoto-Grillot, M. Ducreux, FOLFIRINOX versus gemcitabine for metastatic pancreatic cancer, N. Engl. J. Med. 364 (19) (2011) 1817–1825.
[46] M. Chehelgerdi, M. Chehelgerdi, O.Q.B. Allela, R.D.C. Pecho, N. Jayasankar, D. P. Rao, T. Thamaraikani, M. Vasanthan, P. Viktor, N. Lakshmaiya, M.J. Saadh, A. Amajd, M.A. Abo-Zaid, R.Y. Castillo-Acobo, A.H. Ismail, A.H. Amin, R. Akhavan-Sigari, Progressing nanotechnology to improve targeted cancer treatment: overcoming hurdles in its clinical implementation, Mol. Cancer 22 (1) (2023) 169.
[47] D. Kalyane, N. Raval, R. Maheshwari, V. Tambe, K. Kalia, R.K. Tekade, Employment of enhanced permeability and retention effect (EPR): nanoparticle-based precision tools for targeting of therapeutic and diagnostic agent in cancer, Mater. Sci. Eng. C 98 (2019) 1252–1276.
[48] J. Zhang, P. Zhang, Q. Zou, X. Li, J. Fu, Y. Luo, X. Liang, Y. Jin, Co-delivery of gemcitabine and paclitaxel in cRGD-modified long circulating nanoparticles with asymmetric lipid layers for breast cancer treatment, Molecules 23 (11) (2018).
[49] A. Bhadran, H. Polara, E.L. Calubaquib, H. Wang, G.K. Babanyinah, T. Shah, P. A. Anderson, M. Saleh, M.C. Biewer, M.C. Stefan, Reversible cross-linked thermoresponsive polycaprolactone micelles for enhanced stability and controlled release, Biomacromolecules 24 (12) (2023) 5823–5835.
[50] Y. Di, Y. Gao, X. Gai, D. Wang, Y. Wang, X. Yang, D. Zhang, W. Pan, X. Yang, Co-delivery of hydrophilic gemcitabine and hydrophobic paclitaxel into novel polymeric micelles for cancer treatment, RSC Adv. 7 (39) (2017) 24030–24039.
[51] R.B. Mokhtari, T.S. Homayouni, N. Baluch, E. Morgatskaya, S. Kumar, B. Das, H. Yeger, Combination therapy in combating cancer, Oncotarget 8 (23) (2017).
[52] H. Meng, M. Wang, H. Liu, X. Liu, A. Situ, B. Wu, Z. Ji, C.H. Chang, A.E. Nel, Use of a lipid-coated mesoporous silica nanoparticle platform for synergistic gemcitabine and paclitaxel delivery to human pancreatic cancer in mice, ACS Nano 9 (4) (2015) 3540–3557.
[53] A.M. Shabana, S.P. Kambhampati, R.C. Hsia, R.M. Kannan, E. Kokkoli, Thermosensitive and biodegradable hydrogel encapsulating targeted nanoparticles for the sustained co-delivery of gemcitabine and paclitaxel to pancreatic cancer cells, Int. J. Pharm. 593 (2021) 120139.
[54] W. Yang, Q. Hu, Y. Xu, H. Liu, L. Zhong, Antibody fragment-conjugated gemcitabine and paclitaxel-based liposome for effective therapeutic efficacy in pancreatic cancer, Mater. Sci. Eng., C 89 (2018) 328–335.
[55] L. Liu, P.G. Kshirsagar, S.K. Gautam, M. Gulati, E.I. Wafa, J.C. Christiansen, B. M. White, S.K. Mallapragada, M.J. Wannemuehler, S. Kumar, J.C. Solheim, S. K. Batra, A.K. Salem, B. Narasimhan, M. Jain, Nanocarriers for pancreatic cancer imaging, treatments, and immunotherapies, Theranostics 12 (3) (2022) 1030–1060.
[56] X. Li, X. Peng, M. Zoulikha, G.F. Boafo, K.T. Magar, Y. Ju, W. He, Multifunctional nanoparticle-mediated combining therapy for human diseases, Signal Transduct. Targeted Ther. 9 (1) (2024) 1.